Tumor induction by an endogenous *K-ras* oncogene is highly dependent on cellular context

Carmen Guerra,[1] Nieves Mijimolle,[1] Alma Dhawahir,[1] Pierre Dubus,[2] Marta Barradas,[3,4] Manuel Serrano,[3,4] Victoria Campuzano,[1] and Mariano Barbacid[1,*]

[1]Molecular Oncology Programme, Centro Nacional de Investigaciones Oncológicas (CNIO), Melchor Fernández Almagro 3, 28029 Madrid, Spain
[2]E.A. 2406, Histologie et Pathologie Moléculaire, Université de Bordeaux 2, 33076 Bordeaux, France
[3]Departamento de Inmunología y Oncología, Centro Nacional de Biotecnología, CSIC, Campus de Cantoblanco, 28049 Madrid, Spain
[4]Present Address: Molecular Oncology Programme, Centro Nacional de Investigaciones Oncológicas (CNIO), 28029 Madrid, Spain
*Correspondence: mbarbacid@cnio.es

Summary

We have targeted a *K-ras* allele in mouse embryonic stem (ES) cells to express a K-Ras^{V12} oncoprotein along with a marker protein (β-geo) from a single bicistronic transcript. Expression of this oncogenic allele requires removal of a knocked in STOP transcriptional cassette by Cre recombinase. Primary mouse embryonic fibroblasts expressing this *K-ras*^{V12} allele do not undergo proliferative senescence and proliferate as immortal cells. In mice, expression of *K-ras*^{V12} throughout the body fails to induce unscheduled proliferation or other growth abnormalities for up to eight months. Only a percentage of *K-ras*^{V12}-expressing lung bronchiolo-alveolar cells undergo malignant transformation leading to the formation of multiple adenomas and adenocarcinomas. These results indicate that neoplastic growth induced by an endogenous *K-ras* oncogene depends upon cellular context.

Introduction

Ras genes are some of the most widely studied cancer-related genes due to their frequent activation in human tumors. These prototypic small GTPases act as molecular switches that transfer information from the membrane to the nucleus. Some of their upstream activators include receptor and nonreceptor tyrosine protein kinases and, to a lesser extent, G protein-coupled receptors. Downstream, Ras proteins interact with multiple effector pathways. The best studied are those involved in mitogenic signaling, the Raf/Mek/Erk pathway, and in survival, the phosphoinositol-3 kinase (PI3K)/Pdk/Akt pathway. The structure of Ras proteins, both alone and associated with some of their downstream effectors, has been resolved, thus opening new opportunities for rational drug discovery (Downward, 2003; Vetter and Wittinghofer, 2001).

Among *ras* oncogenes, *K-ras* is the most frequently activated in human tumors. However, its incidence varies widely. Whereas *K-ras* oncogenes are found in almost 90% of pancreatic cancers, they are present in 50% of colon and 25% of lung adenocarcinomas and basically absent from prostate and breast tumors (Bos, 1989). The molecular bases for these variations are unknown. Moreover, its relative contribution to tumor development is still obscure. Whereas in colon adenocarcinomas activation of *K-ras* oncogenes is an early but not an initiating event, in other tumors, activation of *K-ras* oncogenes can be a late event, sometimes associated with invasive or metastatic processes (Bos, 1989).

Unveiling the precise role of *ras* oncogenes in the development of human cancer is hindered by the sporadic nature of their activation and by the fact that tumors grow undetected for several years. The possibility to manipulate the mouse genome has opened new opportunities to develop tumor models that recapitulate more closely those events responsible for the human disease (Fisher et al., 2001; Jackson et al., 2001; Johnson et al., 2001; Meuwissen et al., 2001). In this study, we describe gene-targeted mice in which expression of an endogenous *K-ras* oncogene, engineered by a knockin strategy, can be activated with synthetic steroids at any time and in any tissue. More importantly, expression of this oncogene can be monitored by coexpression of a bicistronic color marker. These mice have allowed us to illustrate that wide expression of an

---

SIGNIFICANCE

Gene-targeted mice described here allow us to monitor the fate of cells expressing an endogenous *K-ras* oncogene in somatic cells. Unexpectedly, most *K-ras* oncogene-expressing cells remain normal for long periods of time (up to eight months), including stem cells that retain their capacity to proliferate and differentiate to form hair follicles in the dermis or intestinal crypts. Only lung bronchiolo-alveolar cells acquire hyperproliferative properties and progress into malignant adenocarcinomas. These observations establish the experimental bases to identify those pathways that convey resistance or permissiveness to *K-ras* transformation within a physiological context. In addition, this work illustrates that an endogenous *K-ras* oncogene, when expressed at physiological levels, does not induce senescence due to oncogenic stress in mouse embryonic fibroblasts (MEFs). Instead, expression of the endogenous *K-ras* oncogene overrides proliferative senescence, a characteristic of immortal cells.
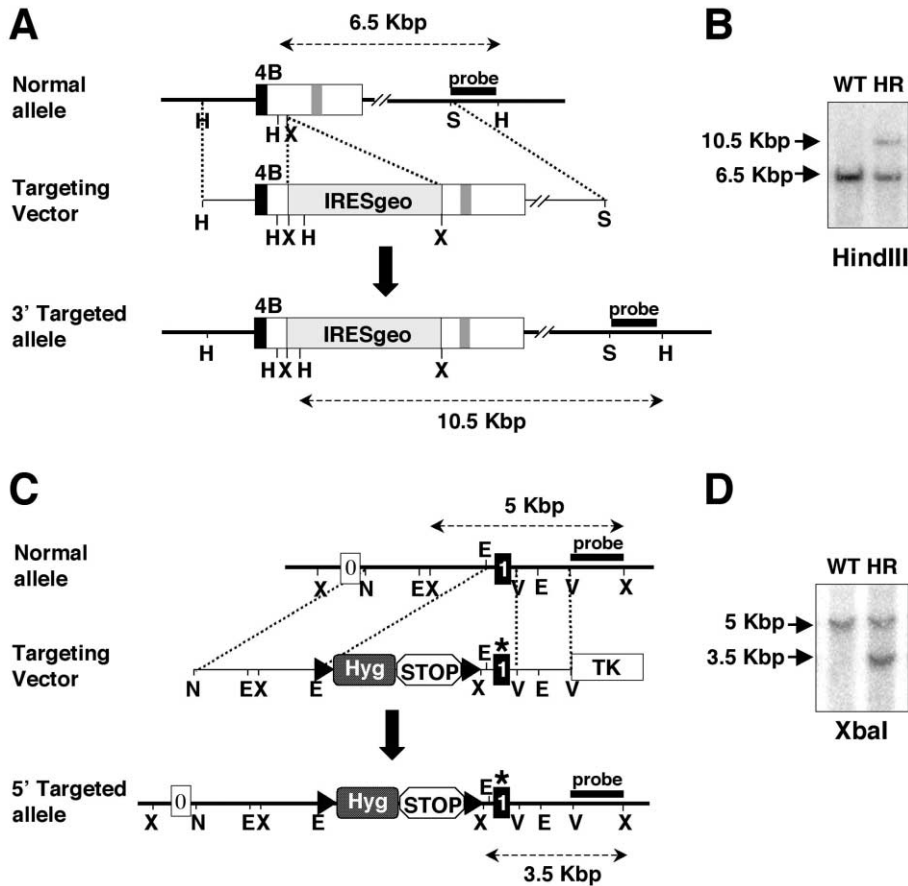

Figure 1. Gene targeting strategy

A: Homologous recombination at the 3' region of the *K-ras* locus. *K-ras* 4B exon: Black, coding sequences; white, noncoding sequences; dark gray, polyadenylation sequences. Light gray, IRES-β-*geo* cassette. The location of the probe used in the Southern blot analysis is indicated. Representative restriction enzyme cleavage sites are indicated (H, HindIII; X, XbaI; S, SalI).

B: Southern blot analysis of DNA isolated from (WT) wild-type and (HR) clones carrying the expected homologous recombination event after digestion with HindIII. The size of the wild-type (6.5 kbp) and targeted (10.5 kbp) alleles is indicated.

C: Homologous recombination at the 5' region of the *K-ras* locus. White box, *K-ras* noncoding exon 0; black box, *K-ras* coding exon 1; Hyg, PGK-Hygromycin cassette; STOP, transcriptional inhibitory sequences; triangle, loxP sites; *, oncogenic mutation in codon 12. The position of the probe used in the Southern blot analysis is indicated. Representative restriction enzyme cleavage sites are indicated (X, XbaI; E, EcoRI; V, EcoRV; N, NotI).

D: Southern blot analysis of DNA isolated from wild-type (WT) and clones (HR) carrying the expected homologous recombination event after digestion with XbaI. The size of the wild-type (5 kbp) and targeted (3.5 kbp) alleles is indicated.

endogenous *K-ras* oncogene has no consequences in most tissues and/or cell types, thus indicating that tumor development is highly dependent on cellular context. Moreover, characterization of mouse embryonic fibroblasts (MEFs) derived from these mice reveals that expression of a *K-ras* oncogene at physiological levels induces cellular immortalization instead of senescence (Serrano et al., 1997).

Results

Targeting strategy

We have targeted mouse embryonic stem (ES) cells to generate an oncogenic *K-ras* allele whose expression can be induced and monitored in vivo. To this end, we introduced by homologous recombination an IRES-β-*geo* cassette within the 3' untranslated region of a *K-ras* allele (Friedrich and Soriano, 1991) (Figure 1A). The internal ribosomal entry site (IRES) allows bicistronic translation of β-*geo* sequences from a transcript driven by the endogenous *K-ras* promoter (Mountford et al., 1994). G418 resistant clones were submitted to Southern blot analysis to identify those that had undergone the expected recombination event (Figure 1B). We obtained a high percentage of homologous recombinant clones (134/192, 70%), most likely due to the lack of an internal promoter in the IRES-β-*geo* cassette. As expected, all G418 resistant clones were positive for X-Gal staining (data not shown). Two clones (MCG224 and MCG231) were selected for a second recombination event in the 5' end of the same *K-ras* allele. This targeting event allowed us to replace the endogenous

first exon with sequences carrying a mutant codon 12 encoding a valine residue, a mutation frequently found in human tumors (Bos, 1989). In this recombination event, we also inserted within the first intron transcriptional STOP sequences (Lakso et al., 1992) and a PGK-Hygro cassette flanked by loxP sites (Figure 1C). Seven out of 96 hygromycin-resistant clones tested (7%) displayed the expected recombination event (Figure 1D).

Targeted ES cells carrying the two recombination events within the same *K-ras* allele (about 50% of the clones) were identified by their ability to express the β-geo marker only upon transfection with Cre recombinase. These cells expressed the targeted *K-ras* mRNA as determined by RT-PCR analysis followed by digestion with a diagnostic SfcI restriction endonuclease as described in Figure 2. Selected clones were submitted to cytogenetic analysis and those that exhibited a normal karyotype (MCG537 and MCG758) were used to generate chimeric mice by microinjection into C57BL/6 blastocysts. Chimeric male mice were backcrossed to C57BL/6 females and germline transmission of the targeted allele scored by Southern blot analysis of tail DNA from the agouti offspring. Heterozygous $K-ras^{+/V12}$ mice were born at the expected Mendelian ratios. These animals do not show obvious abnormalities. X-Gal analysis of embryos and tissues derived from heterozygous $K-ras^{+/V12}$ mice does not reveal cells expressing the β-geo marker. Homozygous $K-ras^{V12/V12}$ embryos die at midgestation with a phenotype similar to that described for $K-ras^{-/-}$ mice (Johnson et al., 1997), indicating that the knocked in transcriptional STOP sequences effectively prevent expression of the $K-ras^{V12}$ allele.
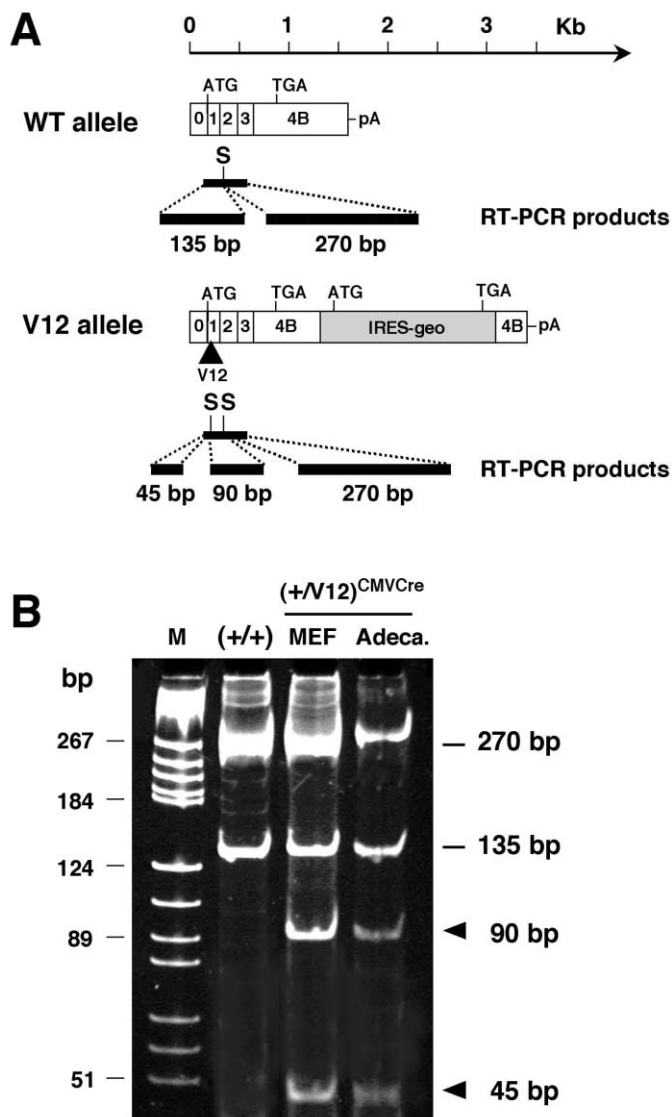
Figure 2. Expression of wild-type and oncogenic *K-ras* alleles

A: Schematic representation of the RT-PCR strategy used to identify transcripts from (WT) wild-type *K-ras* and (V12) oncogenic *K-ras*[V12] alleles. White boxes, *K-ras* transcripts. Numbers indicate exons. Gray box, IRES-β-*geo* sequences present in *K-ras*[V12] transcripts. Translational initiator (ATG) and terminator (TGA) codons, (pA) polyadenosine tail, (V12) oncogenic mutation, and sizes of the RT-PCR products before and after SfcI (S) digestion are indicated.

B: RT-PCR analysis of transcripts present in *K-ras*^{+/+} MEFs, *K-ras*[+/V12]; *CMV-Cre*[+/T] MEFs, and *K-ras*[+/V12];*CMV-Cre*[+/T] lung adenocarcinoma (adeca). Triangles indicate the SfcI DNA fragments (90 bp and 45 bp) diagnostic of the oncogenic *K-ras*[V12] allele.

Expression of an endogenous *K-ras*[V12] oncogene prevents proliferative senescence

We have followed two independent strategies to generate MEFs expressing the oncogenic *K-ras*[V12] allele. First, we obtained MEFs from E13.5 embryos derived from crosses between *K-ras*[+/V12] and *CMV-Cre*[+/T] mice (Figure 3). *CMV-Cre*[+/T] is a transgenic strain that express the Cre recombinase under the control of the CMV viral promoter (Schwenk et al., 1995). All E13.5 *K-ras*[+/V12];*CMV-Cre*[+/T] embryos analyzed were mosaic for β-geo

expression, presumably due to partial excision of the floxed STOP transcriptional sequences. Thus, we treated *K-ras*[+/V12]; *CMV-Cre*[+/T] MEFs with G418 for five days to eliminate those cells not expressing *K-ras*[V12] transcripts.

In addition, we generated MEFs in which the *K-ras*[V12] allele is transcriptionally activated in vitro. To this end, we crossed *K-ras*[+/V12] animals with *RERTn* mice (Figure 3), a knockin strain that expresses the inducible Cre-ERT2 recombinase (Brocard et al., 1997) under the control of the locus encoding the large subunit of RNA polymerase II (V.C., N.M., C.G., and M.B., unpublished data). We treated the resulting *K-ras*[+/V12];*RERTn*[+/ERT] MEFs for six days with 4-hydroxy-tamoxifen (4-OHT) to activate the inducible Cre-ERT2 recombinase and with G418 for five additional days to select for β-geo^{+} cells. The resulting *K-ras*[+/V12]; *RERTn*[+/ERTOHT] MEFs uniformly express the β-geo marker.

MEFs that only express the wild-type *K-ras* allele, including *K-ras*[+/V12], *K-ras*^{+/+};*CMV-Cre*[+/T] and *K-ras*[+/V12];*RERTn*[+/ERT] MEFs, undergo crisis, also known as proliferative senescence, after few passages in culture (Figure 4A). Upon continuous passage, these MEFs become immortal following the same kinetics as *K-ras*^{+/+} MEFs. In contrast, MEFs expressing the oncogenic *K-ras*[+/V12] allele, including *K-ras*[+/V12];*CMV-Cre*[+/T] and *K-ras*[+/V12]; *RERTn*[+/ERTOHT] MEFs, do not undergo proliferative senescence and proliferate continuously as immortal cells (Figure 4A).

Signaling pathways

Proliferating primary *K-ras*[+/V12];*CMV-Cre*[+/T] MEFs contain lower steady-state levels of phosphorylated Erk1/2 proteins than control *K-ras*^{+/+} or *K-ras*[+/V12] MEFs. However, these MEFs exhibit a similar Erk1/2 phosphorylation response upon EGF treatment (Figure 4B). On the other hand, serum-starved primary *K-ras*[+/V12];*CMV-Cre*[+/T] MEFs display a more sustained Erk1/2 phosphorylation in response to EGF than control MEFs (Figure 4C). Sustained activation of the Erk pathway has been associated with cell cycle arrest (Marshall 1995; Agell et al., 2002). However, transient activation of Erk is not sufficient to induce proliferation (Balmanno and Cook, 1999). Moreover, activation of Erk by a constitutively active MAP kinase kinase (Mek1) induces differentiation of PC12 cells but transformation of NIH3T3 cells (Cowley et al., 1994). Thus, the precise levels and duration of Erk1/2 phosphorylation required to elicit specific cellular responses may vary in different cell types. Our results suggest that the sustained activation of Erk1/2 induced by the endogenous *K-ras*[V12] oncogene may be at least partially responsible for the observed loss of proliferative senescence of *K-ras*[+/V12];*CMV-Cre*[+/T] MEFs.

We also observed prolonged activation of downstream kinases in the *ras* survival pathway. As illustrated in Figure 4C, EGF treatment of serum-starved primary *K-ras*[+/V12];*CMV-Cre*[+/T] MEFs maintains detectable levels of phosphorylated Akt kinase for at least one hour, whereas in control MEFs, phosphorylated Akt can no longer be detected 10 min after EGF exposure. Sustained Akt activation may also contribute to loss of proliferative senescence of *K-ras*[V12]-expressing MEFs.

K-ras[V12]-expressing MEFs senesce upon oncogenic stress

Previous studies have indicated that primary MEFs enter a senescence state upon oncogenic stress induced by ectopic expression of *ras* oncogenes (Serrano et al., 1997). These senescent cells display permanent G1 arrest and are phenotypically indistinguishable from those undergoing proliferative senes-

Figure 3. Summary of *K-ras* targeted mice used in this study

Black boxes, *K-ras* coding sequences; white boxes, *K-ras* noncoding sequences; Hyg, PGK-Hygromycin cassette; STOP, transcriptional inhibitory sequences; IRESgeo, IRES-β-*geo* cassette; pA, polyadenylation signal. Triangle, loxP sites. V12, oncogenic mutation in codon 12 that results in replacement of a glycine residue by valine. Arrow, active *K-ras* transcription; X, impaired *K-ras* transcription.

§ In addition to the *K-ras* allele indicated, all strains carry a wild type *K-ras* allele

¶ All strains express the normal K-Ras G12 protein

cence. Since MEFs expressing the K-ras^{V12} allele do not undergo proliferative senescence (Figure 4A), we investigated whether this property could be due to loss of their senescence program. To this end, primary *K-ras$^{+/V12}$;CMV-Cre$^{+/T}$* MEFs were infected with retroviruses carrying *H-ras*, *K-ras4A*, or *K-ras4B* oncogenes. As illustrated in Figure 5A, these MEFs undergo senescence due to oncogenic stress even if they have overriden proliferative senescence. Activation of the senescence program was monitored by expression of their endogenous β-galactosidase (data not shown) and overexpression of Ris1, the product of the *ras-induced senescence* gene, *m-ris1* (Figure 5B) (Barradas et al., 2002). These observations indicate that immortalization induced by the endogenous *K-ras^{V12}* oncogene does not prevent senescence induced by oncogenic stress. These findings suggest that proliferative senescence and senescence induced by oncogenic stress involve different mechanisms.

Transformation of primary MEFs expressing an endogenous *K-ras^{V12}* oncogene

K-ras$^{+/V12}$;CMV-Cre$^{+/T}$ and *K-ras$^{+/V12}$;RERTn$^{+/ERTOHT}$* MEFs show loss of contact inhibition, but do not display the typical morphology of transformed cells. Moreover, they do not grow in semi-solid media and do not form tumors when injected into immuno-compromised mice (data not shown). These MEFs are also resistant to transformation by nuclear oncogenes such as adenovirus *E1A* (Ruley, 1983) (Figure 5C). However, *K-ras$^{+/V12}$; CMV-Cre$^{+/T}$* MEFs undergo morphologic transformation upon cotransfection with exogenous *K-ras* and adenoviral *E1A* oncogenes with efficiencies similar to that of wild-type MEFs (Figure 5C). Transformed *K-ras$^{+/V12}$;CMV-Cre$^{+/T}$* MEFs induce tumors when injected in nude mice with an efficiency similar to wild-type transformed MEFs (data not shown). These results indicate that transformation of primary rodent cells requires the cooperation of two oncogenes, providing that they are expressed at high levels.

Chromosomal abnormalities in late passage *K-ras^{V12}*-expressing MEFs

Overcoming proliferative senescence often involves mutations in either the *INK4a* or *P53* loci. Late passage (p25) *K-ras$^{+/V12}$; CMV-Cre$^{+/T}$* MEFs retain a functional *INK4a* locus, at least as determined by the normal levels of expression of both P16INK4a (not shown) and P19Arf (Figure 5D), the two tumor suppres-

sor proteins encoded by this locus. Likewise, these immortal *K-ras$^{+/V12}$;CMV-Cre$^{+/T}$* MEFs retain a normal P53 pathway as determined by their ability to respond to genotoxic damage. As illustrated in Figure 5D, doxorubicin treatment of passage 25 *K-ras$^{+/V12}$;CMV-Cre$^{+/T}$* MEFs results in the efficient induction of both P53 and P21Cip expression (Figure 5D). These results suggest that immortalization of MEFs expressing an endogenous *K-ras^{V12}* oncogene does not involve loss of tumor suppressor pathways frequently found responsible for the immortalization of normal MEFs in culture.

To investigate whether MEFs expressing the *K-ras^{V12}* oncogene contain other type of mutations such as chromosomal abnormalities, we performed spectral karyotyping analysis (SKY) of primary and late passage (p19) MEFs. Less than 5% of primary *K-ras$^{+/+}$;CMV-Cre$^{+/T}$* and *K-ras$^{+/V12}$;CMV-Cre$^{+/T}$* MEFs display chromosomal abnormalities despite the presence of the *CMV-Cre* transgene (Loonstra et al., 2001). However, as *K-ras$^{+/V12}$;CMV-Cre$^{+/T}$* MEFs proliferate in culture, the number of chromosomal abnormalities increases substantially, reaching up to 50% of the observed metaphases by passage 19. Abnormalities include tetraploidy, reciprocal and unbalanced translocations, deletions, acentric fragments, and dicentric fusions. Parallel cultures of immortal (passage 19) *K-ras$^{+/+}$;CMV-Cre$^{+/T}$* MEFs only display tetraploid cells in 15% of the metaphases analyzed. These results suggest that immortalization induced by expression of the oncogenic *K-ras^{V12}* allele may induce deregulation of checkpoints responsible for maintaining chromosomal stability, thus contributing to tumor development.

Tumor development in *K-ras$^{+/V12}$* mice

Crosses between *K-ras$^{+/V12}$* and *CMV-Cre$^{+/T}$* transgenic mice result in frequent embryonic lethality, presumably due to expression of the *K-ras^{V12}* oncogene during early development (unpublished data). However, a significant number of *K-ras$^{+/V12}$; CMV-Cre$^{+/T}$* mice reach adulthood. These mice develop breathing difficulties after seven to eight months of age (Figure 6, top panel). Postmortem examination reveals a broad spectrum of multifocal lesions in lungs, ranging from small patches of bronchiolo-alveolar hyperplasias to large bronchiolo-alveolar adenomas and adenocarcinomas that compress adjacent lung structures (Figures 6A–6D). These tumor cells express surfactant protein C (SPC), suggesting that they are derived from type II pneumocytes (Figure 6E). Very occasionally, CC10 immuno-
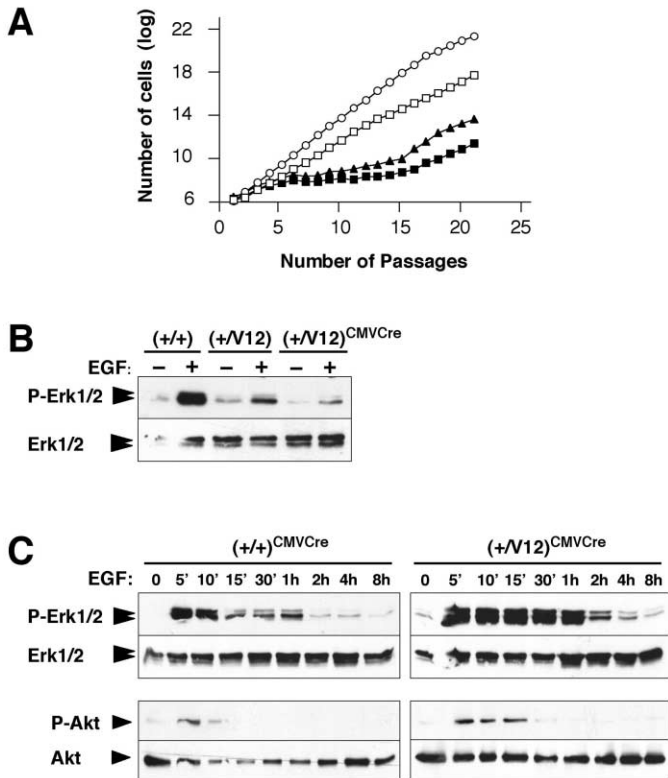
A

B

C

Figure 4. Growth and signaling properties of MEFs expressing an endogenous $K\text{-}ras^{V12}$ oncogene

A: Growth curve of $K\text{-}ras^{+/+}$ (black square), $K\text{-}ras^{+/V12}$ (black triangle), $K\text{-}ras^{+/V12};CMV\text{-}Cre^{+/T}$ (white circle) and $K\text{-}ras^{+/V12};RERTn^{+/ERTOHT}$ (white square) MEFs cultivated according to a 3T3 protocol. The y axis indicates the estimated number of accumulated cells.

B: Western blot analysis of the activation of Erk1/2 in proliferating primary $K\text{-}ras^{+/+}$, $K\text{-}ras^{+/V12}$, and $K\text{-}ras^{+/V12};CMV\text{-}Cre^{+/T}$ MEFs either not treated (−) or treated (+) with 50 ng/ml of EGF for 5 min.

C: Kinetic analysis of the activation of Erk1/2 and Akt kinases upon addition of EGF (50 ng/ml) to serum-starved primary $K\text{-}ras^{+/+};CMV\text{-}Cre^{+/T}$ and $K\text{-}ras^{+/V12};CMV\text{-}Cre^{+/T}$ MEFs. Total Erk1/2 or Akt proteins serve as loading controls.

staining revealed a few cells of Clara cell origin (Figure 6F). These results are similar to those recently reported in other animal models expressing $K\text{-}ras$ oncogenes (Jackson et al., 2001; Johnson et al., 2001; Meuwissen et al., 2001). We have also observed occasional foci of hyperplastic epithelial cells in nonrespiratory bronchioles (data not shown). Tumors other than lung adenomas also appear in these mice, including histiocytic sarcomas (2/20), anal papillomas (3/20), and sarcomas (3/20). All tumors and hyperplastic regions invariably express the β-geo marker (Figures 6A and 6B). Expression of the targeted $K\text{-}ras^{V12}$ allele was confirmed by RT-PCR analysis in selected samples (Figure 2B).

We crossed $K\text{-}ras^{+/V12};CMV\text{-}Cre^{+/T}$ mice with $cdk4^{R24C/R24C}$ knockin animals (Sotillo et al., 2001). $K\text{-}ras^{+/V12};CMV\text{-}Cre^{+/T};cdk4^{+/R24C}$ mice develop multifocal lung adenomas with significantly shorter latency (Figure 6, top panel). These mice also develop histiocytic sarcomas, anal papillomas, and sarcomas. However, the presence of the activated $K\text{-}ras^{V12}$ allele does not accelerate the development of tumors characteristic of $cdk4^{R24C}$

mutant mice, such as pituitary adenomas or hemangiosarcomas (Sotillo et al., 2001), thus suggesting that K-Ras^{V12} signaling in these cells does not contribute to their tumorigenic phenotype (see below). $K\text{-}ras^{+/V12};CMV\text{-}Cre^{+/T};cdk4^{+/R24C}$ mice display focal metaplasia in pancreatic ducts not observed in either parental strain. This metaplasia consists of tall columnar cells with abundant apical mucin, resembling gastric surface epithelial cells (Figure 7). This abnormality closely resembles human mucinous metaplasia (Chen et al., 1985), a preneoplastic lesion that often contains $K\text{-}ras$ oncogenes (Yanagisawa et al., 1993).

Controlled activation of the oncogene $K\text{-}ras^{V12}$ allele in postnatal mice

To activate expression of the $K\text{-}ras^{V12}$ allele in somatic cells in a temporally controlled manner, we submitted P10 $K\text{-}ras^{+/V12};RERTn^{+/ERT}$ mice to systemic treatment involving limiting doses of 4-OHT (0.1 mg, 3 times a week for 2 weeks). Exposure to this synthetic steroid results in the activation of the inducible Cre-ERT2 recombinase leading to removal of the STOP transcriptional sequences that prevent expression of the targeted $K\text{-}ras^{V12}$ allele. X-Gal analysis of tissue sections two weeks after 4-OHT treatment revealed that 5% to 15% of cells in most tissues expressed the β-geo marker (data not shown). After seven months of age (Figure 6, top panel), all treated mice (n = 9) developed breathing difficulties due to the presence of multiple lesions in the lung, indistinguishable from those described above. Southern blot analysis of DNA isolated from lung adenomas reveals that these benign tumors maintain the wild-type allele (data not shown), thus indicating that loss of the normal $K\text{-}ras^{V12}$ allele is not a prerequisite, at least for the early stages of tumor development (Zhang et al., 2001). We have not observed other areas of abnormal growth in these mice, with the exception of hyperplastic Harderian glands.

Histological examination of other tissues obtained from these mice reveals a similar percentage of β-geo$^+$ cells (5% to 15%) as in young mice immediately after 4OHT treatment. These observations suggest that most cells expressing the oncogenic $K\text{-}ras^{V12}$ allele do not have proliferative advantage. Indeed, a significant number of morphologically normal β-geo$^+$ cells, indicative of $K\text{-}ras^{V12}$ expression, could be identified in the bronchiolo-alveolar lung epithelia (Figure 8A). In other tissues, β-geo$^+$ cells appear morphologically normal and within areas completely devoid of any hyperplastic growth (Figures 8B–8H). These tissues include testicular seminiferous tubes (Figure 8B), epithelial cells of the renal Bowman's capsules (Figure 8C), hair follicles in the dermis (some of these being completely made up of β-geo$^+$ cells) (Figure 8D), the molecular layer of the cerebellum (Figure 8E), and liver hepatocytes (Figure 8F). Of particular interest is the presence of morphologically normal β-geo$^+$ cells in the exocrine pancreas (Figure 8G), since most human pancreatic adenocarcinomas contain $K\text{-}ras$ oncogenes (Almoguera et al., 1988). Moreover, these mice contain a significant number of intestinal crypts entirely formed by β-geo$^+$ cells (Figure 8H), suggesting that activation of the $K\text{-}ras^{V12}$ oncogene has occurred in stem cells that retain their full potential to form these crypts. These observations indicate that endogenous $K\text{-}ras^{V12}$ expression does not perturb the proliferation and/or differentiation programs of most cell types.

We observed similar results in $K\text{-}ras^{+/V12};CMV\text{-}Cre^{+/T}$ mice as well as in double mutant $K\text{-}ras^{+/V12};CMV\text{-}Cre^{+/T};cdk4^{+/R24C}$ animals (data not shown). These observations indicate that ex-

A

Vector   K-ras

B

$(+/+)^{CMVCre}$ $(+/V12)^{CMVCre}$

V R   V R V R

Ris1 ►

actin ►

C

D
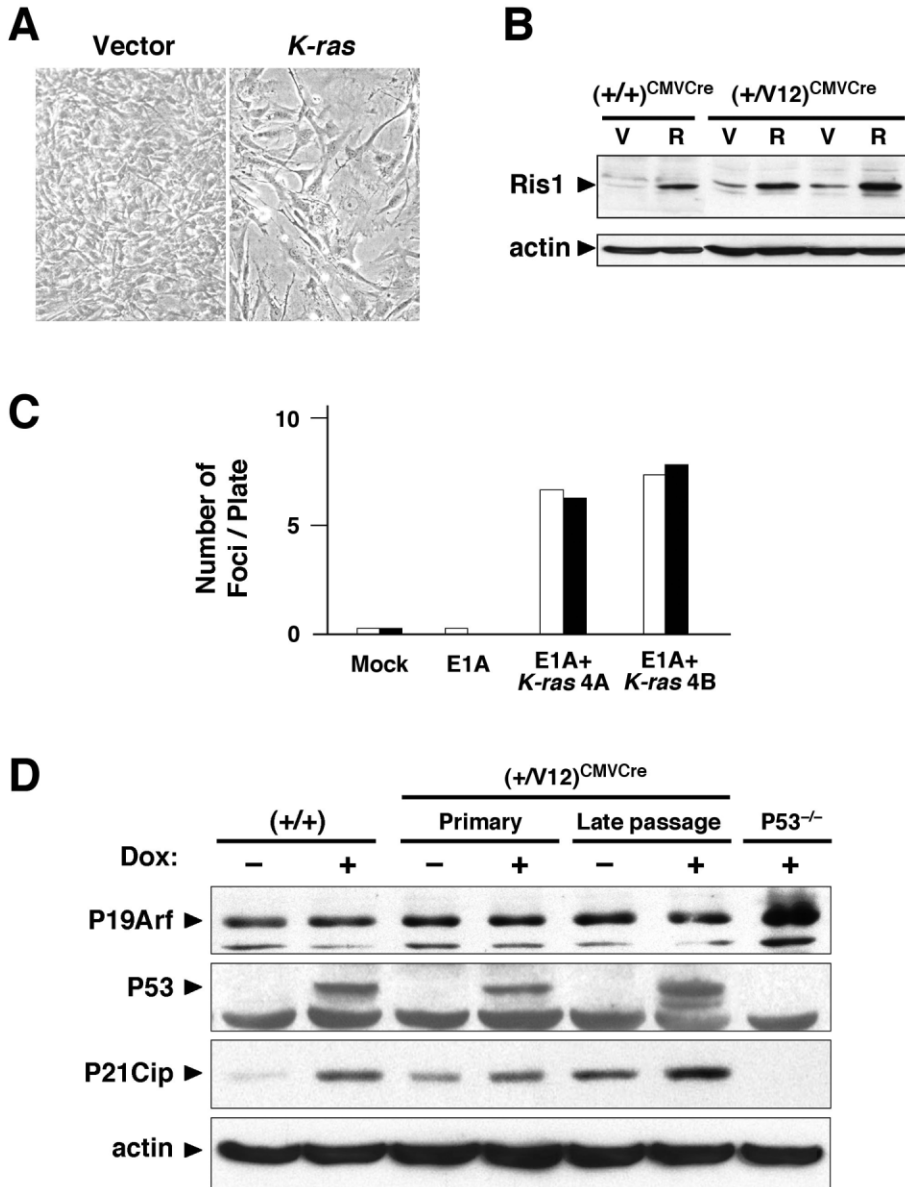

Figure 5. Biological properties of *K-ras*^V12-expressing MEFs

Upper panels: Oncogenic stress induces senescence in *K-ras*^V12-expressing MEFs.

A: Morphology of *K-ras*^+/V12;*CMV-Cre*^+/T MEFs infected with vector alone or with retroviruses carrying the indicated oncogene.

B: Western blot analysis of Ris1 expression in *K-ras*^+/+;*CMV-Cre*^+/T and two independent clones of *K-ras*^+/V12;*CMV-Cre*^+/T MEFs infected with vector alone (V) or with a retrovirus carrying an *H-ras* oncogene (R). β-actin serves as loading control.

Middle panel: Malignant transformation of *K-ras*^V12-expressing MEFs.

C: *K-ras*^+/V12-expressing MEFs can be transformed by ectopic expression of cooperating adenoviral *E1A* and *K-ras* oncogenes

Lower panel: Late passage *K-ras*^+/V12-expressing MEFs retain a functional P53 pathway.

D: Western blot analysis of the expression of P19Arf, P53, and P21Cip in *K-ras*^+/+ MEFs as well as in primary and late passage (p25) *K-ras*^V12; *CMV-Cre*^+/T MEFs either not treated (−) or treated (+) with 0.5 μg/ml of doxorubicin (Dox) for 6 hr. MEFs derived from P53^−/− mice were used as negative controls.

---

pression at physiological levels of even two distinct oncogenic proteins acting in convergent pathways is not sufficient to induce unscheduled proliferation in most cell types.

Discussion

Expression of *ras* oncogenes under the control of retroviral or other highly active promoters in primary MEFs leads to G1 arrest and premature senescence due to oncogenic stress (Serrano et al., 1997). Based on these observations, it was proposed that transformation by *ras* oncogenes requires abrogation of cellular senescence programs, for instance by mutation of the P53 or INK4a tumor suppressor pathways. Here, we show that expression of a targeted *K-ras*^V12 oncogene under the control of its own promoter does not induce senescence, but rather hyperproliferative properties characteristic of immortal cells. Upon

EGF treatment, *K-ras*^V12-expressing MEFs display a more sustained signaling response than control MEFs in their downstream mitogenic (Raf/Mek/Erk) and survival (PI3K/Pdk/Akt) pathways than control MEFs, a trait likely to contribute to their immortal properties. However, expression of the oncogenic *K-ras*^V12 allele at physiological levels is not sufficient to induce morphologic transformation in vitro or tumorigenic properties in vivo, even in the presence of a cooperating oncogene such as *E1A*. Thus, it is likely that if expressed at physiological levels, even rodent MEFs may need multiple mutations to acquire neoplastic properties.

Several in vivo models expressing *K-ras* oncogenes have been recently described (Fisher et al., 2001; Jackson et al., 2001; Johnson et al., 2001; Meuwissen et al., 2001). One of these (Johnson et al., 2001) recapitulates more closely human disease since it involves occasional activation of an endogenous
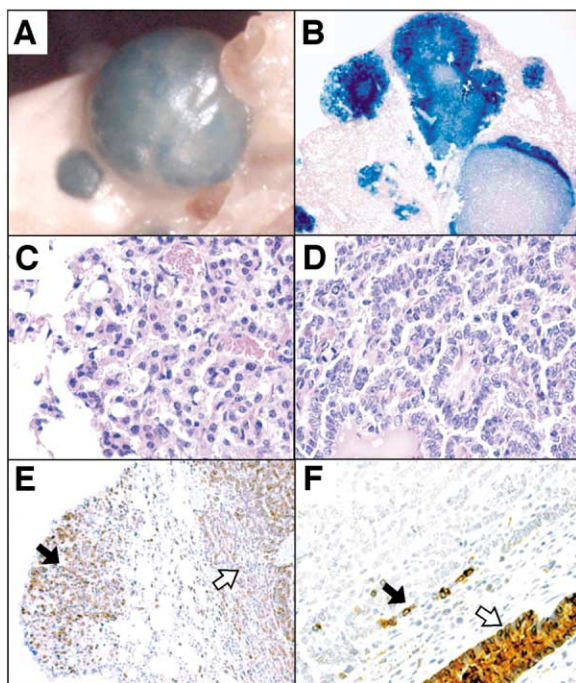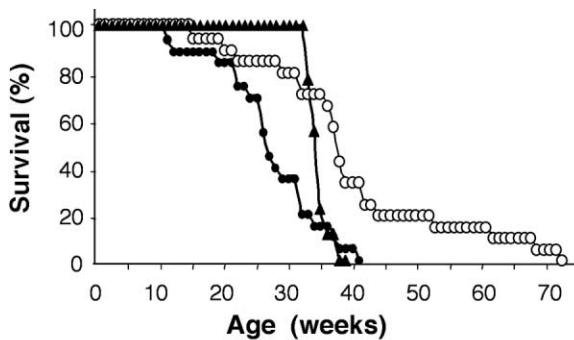
Figure 6. Tumor development in mice expressing *K-ras*[V12] transcripts

Upper panel: Survival curve of *K-ras*[+/V12];*CMV-Cre*[+/T] (white circle), *K- ras*[+/V12]; *CMV-Cre*[+/T];*cdk4*[+/R24C] (black circle), and 4-OHT treated *K-ras*[+/V12];*RERTn*[+/ERT] (black triangle) mice.
Lower panel: Bronchiolo-alveolar tumors in *K-ras*[+/V12];*CMV-Cre*[+/T] mice.
A: Macroscopic view of the lung nodules after whole-mount X-Gal staining.
B: Paraffin section after X-Gal staining of a representative lung with multiple adenomas from a *K-ras*[V12];*CMV-Cre*[+/T] mouse.
C: Alveolar architecture of small adenomas.
D: Morphologic appearance of large adenomas.
E: SP-C immunostaining of a section showing an adenoma (black arrow) and an adenocarcinoma (white arrow).
F: CC10 immunostaining of a section showing an adenoma (black arrow) and a nonrespiratory bronchiole (white arrow).

K-ras oncogene by intragenic recombination in somatic cells. These mice develop lung adenocarcinomas with complete penetrance. Approximately one-third of these mice also develop thymic lymphomas and skin papillomas, as well as aberrant intestinal crypt foci, but no colon tumors. However, this model does not allow identification of those cells expressing the *K-ras* oncogenes or the timing in which *K-ras* activation occurs, thus making it difficult to study the early stages of the disease.

In this study, we have used a targeting strategy similar to that described by Jackson et al. (2001) in which transcription of the targeted *K-ras* allele requires expression of Cre recombinase. In our model, we have activated the *K-ras*[V12] allele by introducing either a *CMV-Cre* transgene that is expressed throughout development or a knocked in inducible Cre-ERT2 recombinase that can be activated at any time in any cell type by exposure to 4-OHT (V.C., N.M., C.G., and M.B., unpublished data). In addition, our targeting strategy allows easy monitoring of those cells expressing the targeted *K-ras*[V12] oncogene by staining for a marker protein (β-geo) expressed from the same *K-ras*[V12] transcript by a bicistronic strategy.

K-ras[+/V12] mice carrying a *CMV-Cre* transgene develop lung adenomas and adenocarcinomas with complete penetrance. About one-third of the animals also develop additional tumors. In contrast, when the targeted *K-ras*[V12] allele is activated postnatally for a short period of time (2 weeks), we observe multifocal lung adenomas and adenocarcinomas, but, so far, no other tumor types. The main difference between these models is that whereas intragenic recombination (Johnson et al., 2001) or *CMV-Cre*-dependent activation (this work) may occur at any time throughout embryonic or postnatal development, 4-OHT-mediated activation of *K-ras*[V12] only takes place for a short period of time. These observations suggest that tumor development induced by endogenous *K-ras* oncogenes is highly dependent not only on the cell type, but also on their developmental and/ or differentiation state when activation occurs.

The inclusion of a marker protein in the knock in strategy has allowed us to establish that expression of the targeted *K-ras*[V12] allele is not limited to those cells that undergo hyperplastic growth or tumor development. On the contrary, *K-ras*[+/V12]; *CMV-Cre*[+/T] and 4-OHT-treated *K-ras*[+/V12];*RERTn*[+/ERT] mice express the oncogenic *K-ras*[V12] allele in a wide range of cell types. However, most of these cells do not display altered morphologies or hyperplastic properties. Examination of young *K-ras*[+/V12]; *CMV-Cre*[+/T] or *K-ras*[+/V12];*RERTn*[+/ERT] mice immediately after 4-OHT treatment reveals a similar percentage of β-geo^{+} cells in lungs as in other tissues in which no tumor development occurs, even after eight months of life. Thus, the high susceptibility of bronchiolo-alveolar cells to tumor development must be due to an intrinsic consequence of their transcriptional program. Whether this is due to a failure of the *K-ras*[V12] oncogene to elicit a mitogenic response or to activation of inhibitory pathways in these cells remains to be explored.

4-OHT-treated *K-ras*[+/V12];*RERTn*[+/ERT] mice contain a significant number of morphologically normal intestinal crypts, entirely made of β-geo^{+} cells. These cells proliferate and differentiate normally despite expressing oncogenic *K-ras*[V12] transcripts. These observations are in agreement with clinical studies that suggest that activation of *K-ras* onogenes is not the primary event in the development of human colon carcinomas (Oudejans et al., 1991). Remarkably, tissues of double mutant *K-ras*[+/V12]; *CMV-Cre*[+/T];*cdk4*[+/R24C] mice also contain a significant percentage of *K-ras*[V12]-expressing cells. These cells also contain a mutant Cdk4[R24C] kinase whose activity cannot be downregulated by INK4 inhibitors. However, none of these tissues display abnormal morphology or hyperproliferative properties, indicating that most cell types tolerate a significant level of oncogenic burden without neoplastic consequences. On the other hand, coexpression of the mutant Cdk4[R24C] protein in bronchiolo-alveolar cells susceptible to transformation by *K-ras*[V12] significantly reduces tumor latency.
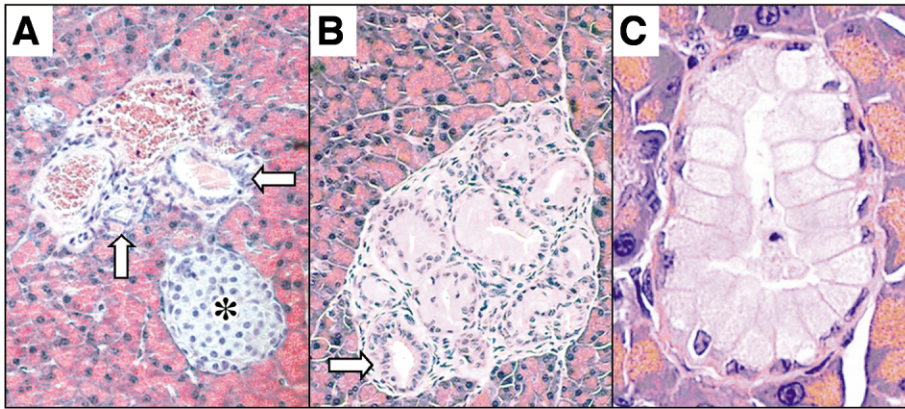
Figure 7. Metaplasia in pancreatic ducts of *K-ras*[+/V12];*CMV-Cre*[+/T];*cdk4*[+/R24C] mice

A: Normal duct. Arrows indicate duct structures. The asterisk indicates an islet.

B: Focal metaplasia in pancreatic ducts. Arrow indicates a normal duct within this abnormal structure.

C: Detailed columnar structure of metaplastic cells with abundant apical mucin resembling gastric surface epithelial cells.

Our results strongly suggest that tumor susceptibility depends to a great extent upon cellular context. Unveiling those pathways responsible for the dramatic differences in the response to *K-ras*[V12] expression in the mice described here should significantly improve our understanding of how neoplastic transformation occurs in vivo.

Experimental procedures

Targeting vectors

K-ras genomic DNA clones were isolated from a 129/Sv genomic DNA library (Stratagene) using as probes a 600 bp EcoRI-HindIII fragment of pSK-*K-ras*

DNA that encompasses the mouse 3′UTR and a 400 bp SacI-StuI fragment of p*CMV-K-ras* DNA that contains the human noncoding exon 0 (Leon et al., 1987). To target the 3′ region of the *K-ras* locus, we generated a targeting vector (pMCG26) by inserting the IRES-β-*geo* cassette (Mountford et al., 1994) into the XbaI site of a 7 Kb HindIII-SalI DNA fragment that encompasses the entire exon 4B. This XbaI site is located 560 bp downstream from the TGA stop codon and 552 bp upstream from a putative polyadenylation site likely to correspond to the 2 Kb *K-ras* transcript (Leon et al., 1987). To target the 5′ region of the *K-ras* locus, we mutagenized two nucleotides (underlined) corresponding to codon 12 (GGT [Gly] to G<u>TA</u> [Val]) in a plasmid containing the first *K-ras* exon within a 700 bp EcoRI DNA fragment. These mutations also create a diagnostic SfcI restriction site, CTG<u>TA</u>G. Selected clones were sequenced to ensure that only the desired mutations were introduced. To
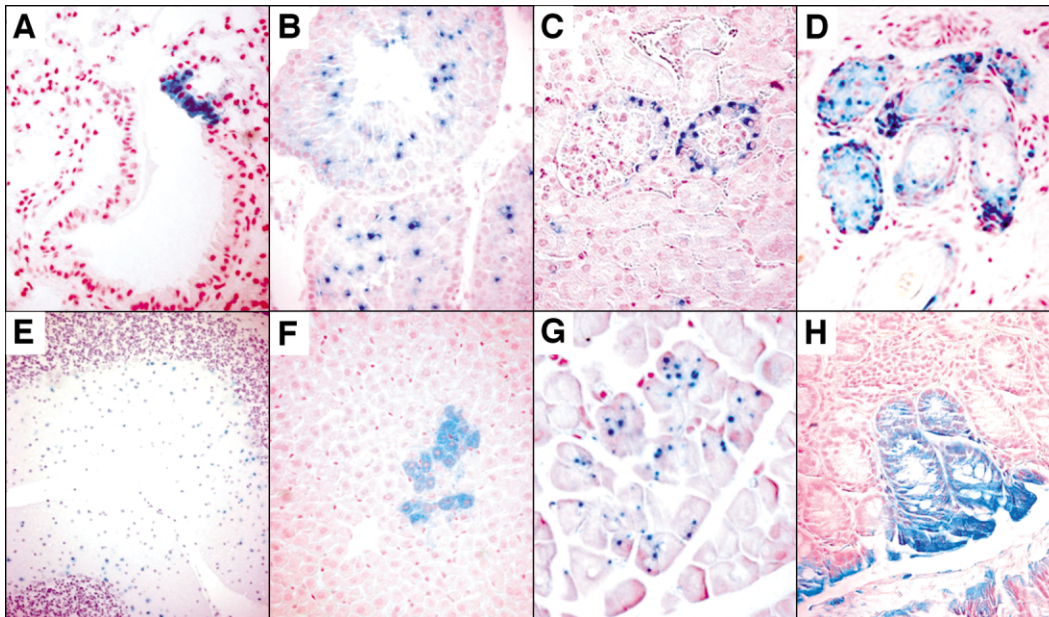

Figure 8. β-geo expression in several tissues of 4-OHT treated *K-ras*[+/V12];*RERTn*[+/ERT] mice

X-Gal staining of representative paraffin sections depicting:

A: Lung bronchiolo-alveolar cells.
B: Testicular seminiferous tubes.
C: Bowman's capsules in the kidney.
D: Hair follicles in the dermis.
E: Molecular layer of the cerebellum.
F: Liver hepatocytes.
G: Exocrine pancreas.
H: Intestinal crypts.

generate the targeting vector (pMCG25), we inserted a PGK-Hyg-STOP cassette flanked by loxP sites within a 5 Kb NotI-EcoRV DNA fragment at an EcoRI site located 100 bp upstream of the mutagenized exon 1. This cassette had been previously generated by inserting a 1.8 Kb BglII DNA fragment containing the hygromycin resistance gene (Hyg) under the control of the phosphoglycerolkinase (PGK) promoter (a gift of Dr. I. Sanchez-García) into the BglII site of pBS302 (Gibco-BRL), a plasmid that contains the floxed STOP sequences.

Generation of knockin mice
R1 ES cells (Nagy et al., 1993) were cultured in Dulbecco's modified Eagle's medium (DMEM) supplemented with 15% heat inactivated fetal bovine serum (FBS) and 10^3 U/ml of leukemia inhibitory factor (LIF). 20 μg of linearized pMCG26 DNA were electroporated into 5.6×10^6 R1 cells in 0.8 ml at 240 V and 500 μF with a Genepulser (BioRad). Cells were grown for 7 days in 200 μg/ml of G418 (Sigma). G418-resistant clones were submitted to Southern blot analysis to identify those that had undergone the expected recombination event. Two clones (MCG224 and MCG231) were selected to target the 5′ region. To this end, 20 μg of linearized pMCG25 DNA was electroporated as described above. Cells were grown for 7 days in 200 μg/ml hygromycin and 2 μM gancyclovir. DNA was isolated from double resistant clones and submitted to Southern blot analysis.

Targeted ES cells carrying the two recombination events in the same allele were identified by X-Gal staining only after transfection with a plasmid encoding a Cre recombinase. Positive clones were submitted to cytogenetic analysis and two of them (MCG537 and MCG758) among those exhibiting a normal karyotype were used to generate chimeric mice by microinjection into C57BL/6 blastocysts. Chimeric male mice were backcrossed to C57BL/6 females and germline transmission of the targeted allele scored by Southern blot analysis of tail DNA from the agouti offspring.

PCR genotyping
For routine genotyping of $K-ras^{+/V12}$ mice, we submitted tail DNA to PCR analysis at 94°C for 5 min, followed by 30 cycles of 94°C denaturing for 1 min, 60°C annealing for 1 min, and 72°C extension for 1 min, followed by an elongation cycle of 72°C for 10 min with the following primers: 5′ forward primer (5I0, 5′-AGGGTAGGTGTTGGGATAGC-3′), reverse wild-type primer (3Ex1, 5′-CTCAGTCATTTTCAGCAGGC-3′), and reverse mutant primer (103rev-2, 5′-CTGCTCTTTACTGAAGGCTC-3′). The sizes of the diagnostic PCR products are 403 bp for the wild-type allele and 621 bp for the targeted $K-ras$ allele. In tissues and MEFs in which the floxed STOP cassette present in the targeted $K-ras$ allele has been excised, primers 5I0 and 3Ex1 yield a DNA fragment of 669 bp.

RT-PCR analysis
To monitor expression of the $K-ras^{V12}$ allele, we isolated RNA form 10^6 $K-ras^{+/V12};CMV-Cre^{+/T}$ (β-geo$^+$ cells) and $K-ras^{+/V12}$ (β-geo$^-$ cells) MEFs using TRIzol reagent (Gibco-BRL) and performed RT-PCR analysis using primers specific for the first and third $K-ras$ exons. First strand cDNA was generated using the GeneAmp RNA PCR Kit (Applied Biosystems). PCR was performed using a forward primer (5′-ACGGAATCCCGTAACTC-3′) derived from exon 1 sequences and a reverse primer (5′-CCTTGCTAACTCCTGAGCC-3′) derived from exon 3 sequences. Conditions for PCR amplification were 94°C for 5 min., followed by 35 cycles of 94°C for 1 min, 60°C for 1 min, and 72°C for 1 min, followed by an elongation cycle of 72°C for 7 min. PCR products were digested for 1 hr at 37°C with SfcI and analyzed in 10% polyacrilamide gels.

To separate β-geo$^+$ and β-geo$^-$ cells, we mechanically disaggregated fresh tissues with a Medimachine (DakoCytomation), submitted to the C12-FDG (Molecular Probes) protocol (Plovins et al., 1994) and sorted (MoFlo system, DakoCytomation). Total RNA was purified from 2×10^6 β-geo$^+$ and β-geo$^-$ sorted cells using TRIzol reagent (Gibco-BRL) and submitted to RT-PCR analysis as indicated above.

Cell culture assays
We isolated and propagated MEFs from E13.5 embryos using a classical 3T3 protocol (Todaro and Green, 1963). $K-ras^{+/V12};CMV-Cre^{+/T}$ MEFs were treated with 200 μg/ml of G418 for five days. $K-ras^{+/V12};RERTn^{+/ERT}$ MEFs were treated with 0.5 μM 4-OHT (Sigma) followed by treatment with 800 μg/ml of G418 for five days. For senescence assays, we infected 8×10^5 MEFs with recombinant retroviruses expressing $H-ras$, $K-ras4A$, and $K-ras4B$

oncogenes and selected in the presence of 2 μg/ml of puromycin for 3 days (Serrano et al., 1997). For transformation assays, we transfected primary MEFs (passage 3) by the standard calcium chloride protocol with pMCV-E1A12S (Kraus et al., 1992) and pBABE-puro-$K-rasA^{V12}$ or pBABE-puro-$K-rasB^{V12}$ DNAs. We scored foci of morphologically transformed cells after 20 days in culture. For tumorigenesis assays, foci were inoculated in the flank of nude mice (10^6 cells per flank). Mice were sacrificed when tumors reached a diameter of 1 cm.

Western blot analysis
Tissue samples or cultured cells were lysed in 50 mM Tris-HCl (pH 7.4) containing 150 mM NaCl, 0.5% NP-40, and protease inhibitors. Extracts were separated by 12% or 15% SDS-PAGE, transferred to nitrocellulose filters, and incubated with the corresponding antibodies including anti-Erk (sc-94, Santa Cruz Biotechnology), anti-P-Erk, anti-P-Akt, anti-Akt (9019S, 9271S, 9272, respectively, New England Biolabs), anti-Ris1, anti P19Arf (ab80, Abecam), anti-P53 (Ab3, Oncogene Research Products), anti-P21Cip (sc-397G, Santa Cruz Biotechnology), and β-actin (AC-15, Sigma). Antibodies were detected with the appropriate horseradish peroxidase-linked secondary antibody and visualized with enhanced chemioluminiscent (ECL) system (Amersham).

Spectral karyotyping (SKY)
Painting probes for each chromosome were generated from flow-sorted mouse chromosomes using sequence-independent DNA amplification. Labeling was performed by incorporating four different dyes in a combination sequence that allows unique and differential identification of each chromosome. To obtain mouse metaphases, MEF cultures were exposed to colcemid for 3 hr, treated for 20 min in isotonic conditions (70 mM KCl), washed three times in Carnoy's fixative (methanol:acetic acid, 3:1), and dropped into glass slides. Prior to hybridization, chromosome spreads were treated with pepsin (0.001% pepsin in 10 mM HCl, 37°C). A mouse SKY probe mixture (Applied Spectral Imaging) was hybridized for 48 hr. Washing of preparations and detection of probe was carried out according to the instructions of the manufacturer. Chromosome spreads were counterstained with DAPI. Image acquisition was performed with the SpectraCube system (Applied Spectral Imaging) mounted on an Axioplan 2 microscope (Zeiss).

Histological analysis, X-Gal staining, and immunohistochemistry
Mice were sacrificed at the specified times or upon onset of visible disease. Tissue samples were fixed in 10% formalin and processed for hematoxylin and eosin (H&E) staining. X-Gal staining was performed as described (Hogan et al., 1994). Counterstaining of paraffin sections was performed with nuclear fast red. Antibodies against SP-C (AB3786, Chemicon) and CC10 (sc-9772, Santa Cruz Biotechnology) were used at a final dilution of 1:500.

References

Agell, N., Bachs, O., Rocamora, N., and Villalonga, P. (2002). Modulation of the Ras/Raf/MEK/ERK pathway by Ca(2+), and calmodulin. Cell. Signal. *14*, 649–654.

Almoguera, C., Shibata, D., Forrester, K., Martin, J., Arnheim, N., and Perucho, M. (1988). Most human carcinomas of the exocrine pancreas contain mutant c-K-ras genes. Cell *53*, 549–554.

Balmanno, K., and Cook, S.J. (1999). Sustained MAP kinase activation is required for the expression of cyclin D1, p21Cip1 and a subset of AP-1 proteins in CCL39 cells. Oncogene *18*, 3085–3097.

Barradas, M., Gonos, E.S., Zebedee, Z., Kolettas, E., Petropoulou, C., Delgado, M.D., Leon, J., Hara, E., and Serrano, M. (2002). Identification of a candidate tumor-suppressor gene specifically activated during Ras-induced senescence. Exp. Cell Res. *273*, 127–137.

Bos, J.L. (1989). ras oncogenes in human cancer: a review. Cancer Res. *49*, 4682–4689.

Brocard, J., Warot, X., Wendling, O., Messaddeq, N., Vonesch, J.L., Chambon, P., and Metzger, D. (1997). Spatio-temporally controlled site-specific somatic mutagenesis in the mouse. Proc. Natl. Acad. Sci. USA *94*, 14559–14563.

Cowley, S., Paterson, H., Kemp, P., and Marshall, C.J. (1994). Activation of MAP kinase kinase is necessary and sufficient for PC12 differentiation and for transformation of NIH 3T3 cells. Cell *77*, 841–852.

Chen, J., Baithun, S.I., and Ramsay, M.A. (1985). Histogenesis of pancreatic carcinomas: a study based on 248 cases. J. Pathol. *146*, 65–76.

Downward, J. (2003). Targeting Ras signalling pathways in cancer therapy. Nat. Rev. Cancer *3*, 11–22.

Fisher, G.H., Wellen, S.L., Klimstra, D., Lenczowski, J.M., Tichelaar, J.W., Lizak, M.J., Whitsett, J.A., Koretsky, A., and Varmus, H.E. (2001). Induction and apoptotic regression of lung adenocarcinomas by regulation of a K-Ras transgene in the presence and absence of tumor suppressor genes. Genes Dev. *15*, 3249–3262.

Friedrich, G., and Soriano, P. (1991). Promoter traps in embryonic stem cells: a genetic screen to identify and mutate developmental genes in mice. Genes Dev. *5*, 1513–1523.

Hogan, B., Beddington, R., Costantini, F., and Lacy, E. (1994). Manipulating the Mouse Embryo: A Laboratory Manual, Second edition (Cold Spring Harbor, NY: Cold Spring Harbor Laboratory Press).

Jackson, E.L., Willis, N., Mercer, K., Bronson, R.T., Crowley, D., Montoya, R., Jacks, T., and Tuveson, D.A. (2001). Analysis of lung tumor initiation and progression using conditional expression of oncogenic K-ras. Genes Dev. *15*, 3243–3248.

Johnson, L., Greenbaum, D., Cichowski, K., Mercer, K., Murphy, E., Schmitt, E., Bronson, R.T., Umanoff, H., Edelmann, W., Kucherlapati, R., and Jacks, T. (1997). K-ras is an essential gene in the mouse with partial functional overlap with N-ras. Genes Dev. *11*, 2468–2481.

Johnson, L., Mercer, K., Greenbaum, D., Bronson, R.T., Crowley, D., Tuveson, D.A., and Jacks, T. (2001). Somatic activation of the K-ras oncogene causes early onset lung cancer in mice. Nature *410*, 1111–1116.

Kraus, V.B., Moran, E., and Nevins, J.R. (1992). Promoter-specific transactivation by the adenovirus E1A12S product involves separate E1A domains. Mol. Cell. Biol. *12*, 4391–4399.

Lakso, M., Sauer, B., Mosinger, B., Jr., Lee, E.J., Manning, R.W., Yu, S.H.,

Mulder, K.L., and Westphal, H. (1992). Targeted oncogene activation by site-specific recombination in transgenic mice. Proc. Natl. Acad. Sci. USA *89*, 6232–6236.

Leon, J., Guerrero, I., and Pellicer, A. (1987). Differential expression of the ras gene family in mice. Mol. Cell. Biol. *7*, 1535–1540.

Loonstra, A., Vooijs, M., Beverloo, H.B., Allak, B.A., van Drunen, E., Kanaar, R., Berns, A., and Jonkers, J. (2001). Growth inhibition and DNA damage induced by Cre recombinase in mammalian cells. Proc. Natl. Acad. Sci. USA *98*, 9209–9214.

Marshall, C.J. (1995). Specificity of receptor tyrosine kinase signaling: transient versus sustained extracellular signal-regulated kinase activation. Cell *80*, 179–185.

Meuwissen, R., Linn, S.C., van der Valk, M., Mooi, W.J., and Berns, A. (2001). Mouse model for lung tumorigenesis through Cre/lox controlled sporadic activation of the K-Ras oncogene. Oncogene *20*, 6551–6558.

Mountford, P., Zevnik, B., Duwel, A., Nichols, J., Li, M., Dani, C., Robertson, M., Chambers, I., and Smith, A. (1994). Dicistronic targeting constructs: reporters and modifiers of mammalian gene expression. Proc. Natl. Acad. Sci. USA *91*, 4303–4307.

Nagy, A., Rossant, J., Nagy, R., Abramow-Newerly, W., and Roder, J.C. (1993). Derivation of completely cell culture-derived mice from early-passage embryonic stem cells. Proc. Natl. Acad. Sci. USA *90*, 8424–8428.

Oudejans, J.J., Slebos, R.J., Zoetmulder, F.A., Mooi, W.J., and Rodenhuis, S. (1991). Differential activation of ras genes by point mutation in human colon cancer with metastases to either lung or liver. Int. J. Cancer *49*, 875–879.

Plovins, A., Alvarez, A.M., Ibañez, M., Molina, M., and Nombela, C. (1994). Use of fluorescein-di-beta-D-galactopyranoside (FDG) and C12-FDG as substrates for beta-galactosidase detection by flow cytometry in animal, bacterial, and yeast cells. Appl. Environ. Microbiol. *60*, 4638–4641.

Ruley, H.E. (1983). Adenovirus early region 1A enables viral and cellular transforming genes to transform primary cells in culture. Nature *304*, 602–606.

Schwenk, F., Baron, U., and Rajewsky, K. (1995). A cre-transgenic mouse strain for the ubiquitous deletion of loxP-flanked gene segments including deletion in germ cells. Nucleic Acids Res. *23*, 5080–5081.

Serrano, M., Lin, A.W., McCurrach, M.E., Beach, D., and Lowe, S.W. (1997). Oncogenic ras provokes premature cell senescence associated with accumulation of p53 and p16INK4a. Cell *88*, 593–602.

Sotillo, R., Dubus, P., Martin, J., de la Cueva, E., Ortega, S., Malumbres, M., and Barbacid, M. (2001). Wide spectrum of tumors in knock-in mice carrying a Cdk4 protein insensitive to INK4 inhibitors. EMBO J. *20*, 6637–6647.

Todaro, G.J., and Green, H. (1963). Quantitative studies of the growth of mouse embryo cells in culture and their development into stablish lines. J. Cell Biol. *17*, 299–313.

Vetter, I.R., and Wittinghofer, A. (2001). The guanine nucleotide-binding switch in three dimensions. Science *294*, 1299–1304.

Yanagisawa, A., Ohtake, K., Ohashi, K., Hori, M., Kitagawa, T., Sugano, H., and Kato, Y. (1993). Frequent c-Ki-ras oncogene activation in mucous cell hyperplasias of pancreas suffering from chronic inflammation. Cancer Res. *53*, 953–956.

Zhang, Z., Wang, Y., Vikis, H.G., Johnson, L., Liu, G., Li, J., Anderson, M.W., Sills, R.C., Hong, H.L., Devereux, T.R., et al. (2001). Wildtype Kras2 can inhibit lung carcinogenesis in mice. Nat. Med. *29*, 25–33.